Mechanical Science Reports

Improved corrosion resistance Zr-2Ag alloy doped with Co element for biomaterial screw dental implant

Diah Gustanti[a], Muki Satya Permana[b], Djoko Hadi Prayitno[c], Turnad Lenggo Ginta[d], S. Sugiharto[e]
[a,b,e] Universitas Pasundan Bandung, Indonesia

[c] Research Organization for Nuclear Energy-National Research and Innovation Energy, BRIN
Bandung, Indonesia

[d] Research Centre for Process and Manufacturing Industry Technology, BRIN
Serpong, Indonesia

Email of the corresponding author: muki.satya@unpas.ac.id

Abstract

Implant materials offer a promising avenue for addressing human organ damage or dysfunction. The diverse requirements associated with implants or biomaterials drive ongoing research efforts. One critical criterion for implant materials is robust corrosion resistance to mitigate the risk of rejection within the body. This study aims to evaluate the corrosion behavior of Zr-Ag-Co implant material in lactated Ringer's solution. Zr-Ag-Co implant material, with 5% and 7.5% Co content, was synthesized via a melting process utilizing a Single Arc Melting Furnace under an argon gas atmosphere. The synthesized materials were characterized using optical microscopy and Vickers hardness testing. Corrosion behaviour was assessed employing a potentiostat with the Tafel polarization method in Ringer's lactate solution. Optical microscopy and X-ray diffraction (XRD) analysis revealed the presence of phases such as -Zr and -Zr, along with intermetallic compounds Zr_2Co and Zr2Ag. Hardness testing indicated that the increase of Co content led to elevated hardness values for the Zr-Ag-Co alloy, ranging from 496.87 to 510.44 HV.

Keywords: corrosion resistance, implant material, Ringer's lactate solution, Tafel polarization, Zr-Ag-Co

1. Introduction

Dental problems have caused health problems as teeth decay becomes a breeding place for bacteria that cause further health problems [1]. Dental caries can lead to tooth loss, necessitating immediate restoration to restore normal function and prevent further decay [2]. The advanced dental technology for dental caries has arisen. The use of dental implants for solving dental health problems has been proposed and developed in research. Finding the appropriate and safe material for dental implants is a concern in material engineering [2], [3], [4]. Dental screw material is a method for addressing tooth loss through the use of dental implants, which provide support for dentures [5], [6]. Dental implants come into direct contact with bodily tissues, necessitating materials with biocompatibility, strength to withstand chewing forces, corrosion resistance, and fracture resistance [7], [8], [9].

The development of dentistry leads to advanced research on dental implant materials. Years of dental problems solutions for teeth problems, especially cavities, have selected metals, ceramics, and polymers for dental implants [10], [11], [12]. Those are chosen for their mechanical strength, durability, biocompatibility, and wear resistance. Metallic materials for dental implants, including cobalt-chromium alloys, stainless alloy, and titanium and its alloys, are used as prosthetic frames, implants, metal covers under ceramic crowns, and dental braces [13], [14], [15]. Among the metallic materials, Ti-6Al-4V is a commonly used dental implant material due to its biocompatibility, allergy resistance, and corrosion resistance [16], [17], [18], [19]. However, its high-cost prompts exploration of alternative materials.

Zirconium-based dental implant materials present promising alternatives, offering excellent biomechanical properties, biocompatibility, and corrosion resistance [20], [21], [22]. It is required for surface modifications, including roughening, surface activation, and coating. The adoption of zirconium in dental implants is justified by its mechanical, aesthetic, and excellent biological properties [23], [24]. Its naturally white colour imitates the natural teeth colour and avoids the blurring to grey colour of soft tissue that sometimes occurs in titanium implants. Depending on the doping concentration and processing conditions, silver-doped zirconia exhibits comparable or slightly reduced flexural strength compared to pure zirconia. A study found that doping zirconia with silver at specific molar ratios resulted in materials with sufficient strength for dental applications [25], [26], [27], [28]. Moreover, the addition of silver to zirconium affects zirconium's toughness and hardness [29].

This study proposes combining Zirconium with Cobalt and Silver. Cobalt is selected for its corrosion and wear resistance, and is commonly used in dental implants and artificial joints [30], [31], [32]. Argentum or silver is included for its antibacterial properties [33], [34], [35]. This research aims to investigate the properties of Zr-Ag-Co alloy as a potential replacement for Ti-6Al-4V in screw dental implants. The study will employ casting methods and characterize the material through visual tests, hardness testing, microstructure analysis, X-ray diffraction, scanning electron microscopy (SEM), and corrosion rate measurement using the Tafel polarization method in simulated body fluid (SBF) solution.

2. Methods

The adoption of zirconium with cobalt and silver for dental implants was conducted with experimental methods. The raw materials of the alloy were melted using an Arc Furnace located in the Physics Laboratory of PSTNT Batan Bandung because zirconium has a relatively high melting point. The principle of operation of the Single Arc Melting Furnace involves melting using a Tungsten (W) electrode supplied with electric current from a generator with a voltage of 230 V and a current of 110 A, resulting in an arc that melts the material inside a copper crucible hearth cooled by circulating water. The melting process is carried out in an Argon gas atmosphere with a controlled height, aiming to protect the melted material from oxidation. The materials utilized and the laboratory tests conducted are outlined in Table 1.

Table 1. The materials used and the laboratory tests

No.	Zr	Ag	Co	Microstructure	XRD	SEM/EDS	Hardness
1	98	Balance	0	✓	✓	✓	✓
2	93		5				
3	90,5		7,5				

3. Results and Discussions

Visual Inspection

The experiment results are the number of data, i.e. images, graphs, visual inspection, metallographic testing, hardness testing, phase or compound testing (XRD), measurement of solution pH, corrosion testing, Scanning Electron Microscope (SEM) and Energy Dispersive Spectroscopy (EDS) testing as well as bacterial testing.

Figure 1. Results of Visual Examination After Smelting Process (a) Specimen 1 (Zr-2Ag), (b) Specimen II (Zr-2Ag-5Co), and (c) Specimen III (Zr-2Ag-7.5Co)

Specimens made through the melting process using a Single Arc Melting Furnace are visually examined by documenting their surface morphology using a digital camera. This examination was conducted to determine the surface image of the specimen. The first specimen was dark grey and matte, the second specimen was bluish and glossy, while the third specimen was golden and glossy. Colour differences may occur due to differences in the cleanliness conditions of the tip of the electrode used during the smelting process.

The specimen was shaped into a cylinder with a diameter of 15 mm with a thickness of ± 4 mm to facilitate the characterisation process. It was conducted before the characterisation process.

(a) (b) (c)

Figure 2. Visual Examination Results Before Characterisation Process (a) Specimen I (Zr-2Ag), (b) Specimen II (Zr-2Ag-5Co), and (c) Specimen 111 (Zr-2Ag-7.5Co)

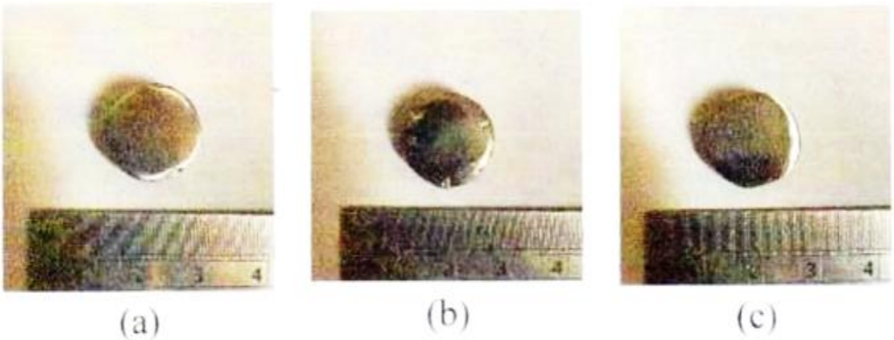

Figure 3. Visual Examination Results After Characterisation Process (a) Specimen 1 (Zr-2Ag). (b) Specimen II (Zr-2Ag-5Co). and (c) Specimen III (Zr-2Ag-7,5Co)

Specimens before characterization were grey and not shiny. Then the specimen undergoes a sanding process from 80 mesh to 2000 mesh until the color changes to a glossier finish before finally going through the metallographic inspection process, hardness testing, and corrosion testing. The $\pm$ 10 mm^2 of the specimen, which was in direct contact with the test media solution, had changed in color after the corrosion test, while the part that was retained by the holder remained shiny.

Metallographic Observation

Based on the metallographic examination in Figure 4-6, the microstructure obtained is dendritic in shape. It shows the results of the casting process. In the microstructure produced from the Zr-2Ag alloy, the -Zr phase is found as a matrix, and the -Ti phase is marked by the bright part above the needle-shaped matrix. Meanwhile, in the Zr-2Ag-5Co and Zr-2Ag-7.5Co alloys, intermetallic compounds such as Ti-Cu and Zr-Cu were found, which were characterized by white spots on the matrix and blackish colour at the grain boundaries.

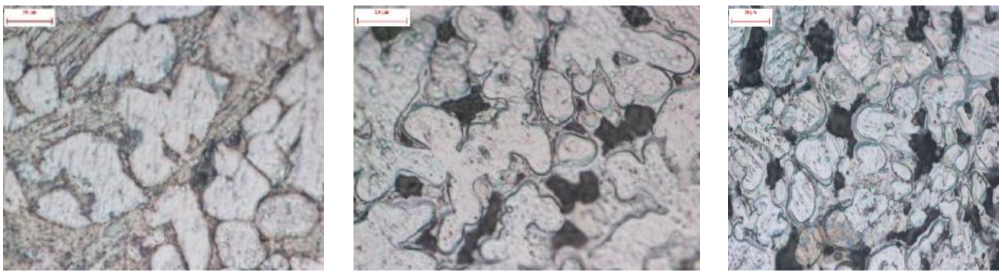

(a) (b) (c)

Figure 4. Metallographic Examination Results with 20 m Magnification (a) Specimen 1 (Zr-2Ag), (b) Specimen II (Zr-2Ag-5Co), and (c) Specimen III (Zr-2Ag-7.5Co)

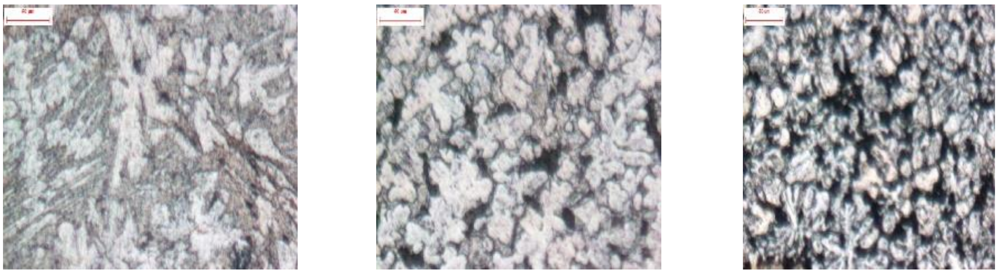

(a) (b) (c)

Figure 5. Metallographic Examination Basil with 40 m Magnification (a) Specimen I (Zr-2Ag), (b) Specimen 11 (Zr-2Ag-5Co), and (c) Specimen 111 (Zr-2Ag-7.5Co)

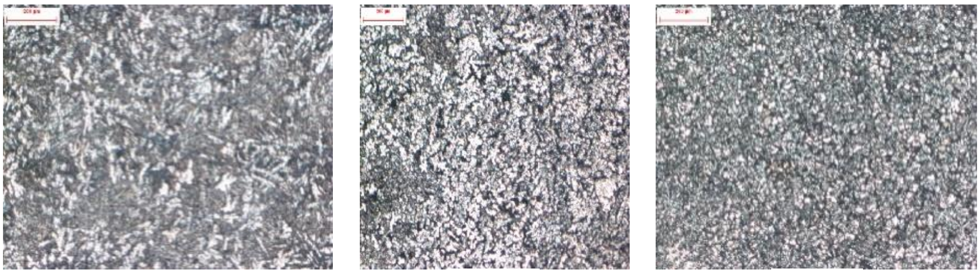

(a) (b) (c)

Figure 6. Results of Metallographic Examination with a Magnification of 200 m (a) Specimen 1 (Zr-2Ag), (b) Specimen FI (Zr-2Ag-5Co), and (c) Specimen II (Zr-2Ag-7.5Co)

Vickers Hardness Test

The next test was the hardness test using the Vickers method. It was conducted at the Metallurgy & Bonding Composite Laboratory of PT. Indonesian Aerospace. This hardness test aims to determine the hardness value of each specimen. The average value data that has been obtained is then converted into a graph to show the effect of the addition of Cobalt on the hardness of the Zr-2Ag alloy. Based on the data from the hardness test results using the Vickers method in Table 2 the test specimen with the composition Zr-2Ag-7.5Co has the highest average hardness value and the lowest average hardness value is owned by the Zr-2Ag specimen. This can indicate that the addition of Cobalt (Co) in the Zr-2Ag alloy affects the hardness value.

Table 2. Vickers Hardness Number

Test Point	Hardness Vickers (HV)		
	Zr-2Ag alloy	Zr-2ag-5Co alloy	Zr-2Ag-7.5Co alloy
1st	477	495	523
2nd	460	513	508
3rd	468	486	505
4th	476	490	504
5th	485	501	513
Average	474	499	510

X-Ray Diffraction (XRD) Test Result

Figure 7 shows the diffraction of a sample of 98Zr, which was analysed by Rietveld using the GSASS II software, showing peaks corresponding to the peak patterns of alpha Zr and Beta Zr using the CIF database 9008559 for Beta Zr and 9008523 for Alpha Zr.

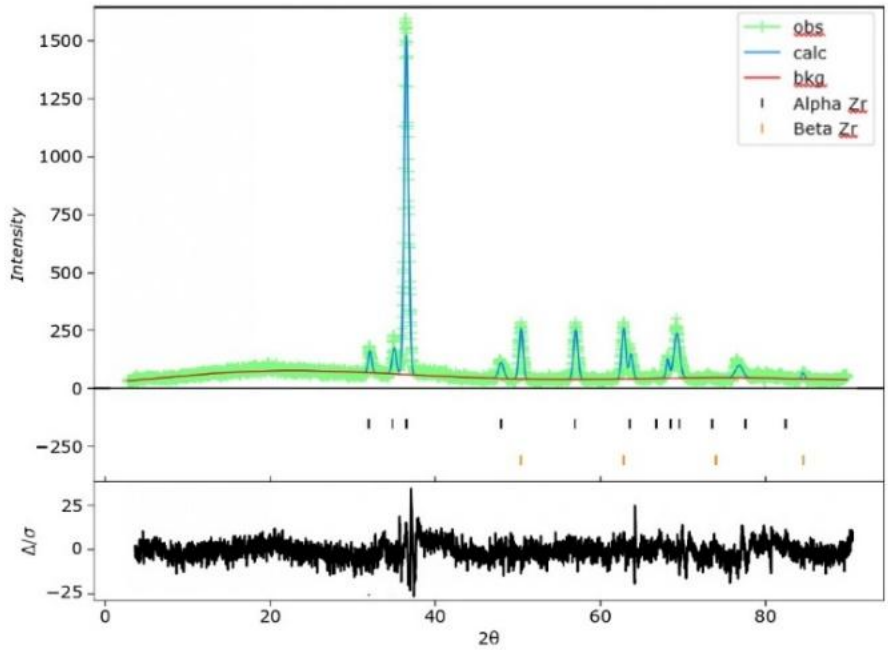

Figure 7. XRD results from a sample of 98% Zr, analysed by Rietveld using GSAS II software

The data from the Rietveld analysis were then processed into 3D images of the Alpha Zr and Beta Zr structures using VESTA software. For this image, Alpha Zr forms a hexagonal structure with a P63/mmc space group, while the Beta Zr phase forms a cubic structure with an Im-3m space group. In addition, it appears that the first sample formed another phase besides Alpha Zr, namely Beta Zr, which is indicated by the orange line. While the model used has a value of Goodness of Fit (GOF) = 1.25 and wR = 5.666. The results of the calculation of the weight fraction of the first sample using GSAS-II are shown in Table 3.

Table 3. ZrAg sample weight fraction

Phase	% Fraction
Alpa Zr	80.3%
Beta Zr	19.7%

In the further test, it discusses two samples consisting of two types of variations, namely variations in the addition of Co doping to the ZrAg sample. The first sample is Zr92%Ag3%Co5% sample, which is synthesized with a stoichiometric ratio with the casting process at a temperature of 2000°C for 10 minutes, with cooling for 15 minutes. The aim is to add Co elements so that more secondary phases are formed during the sintering process. Rietveld refinement results using GSAS-II (Figure 8). From Fig. 8, it can be seen that the first sample is almost obtained with ZrAgMo samples, but it is still followed by two phases, namely alpha Zr which is indicated by a dark blue line and beta Zr phase which is indicated by a red line. The results of this first sample refinement show that the model used has a Goodness of Fit (GOF) = 1.48 and wR = 5.464. Meanwhile, the results of the weight fraction calculation are shown in Table 4.

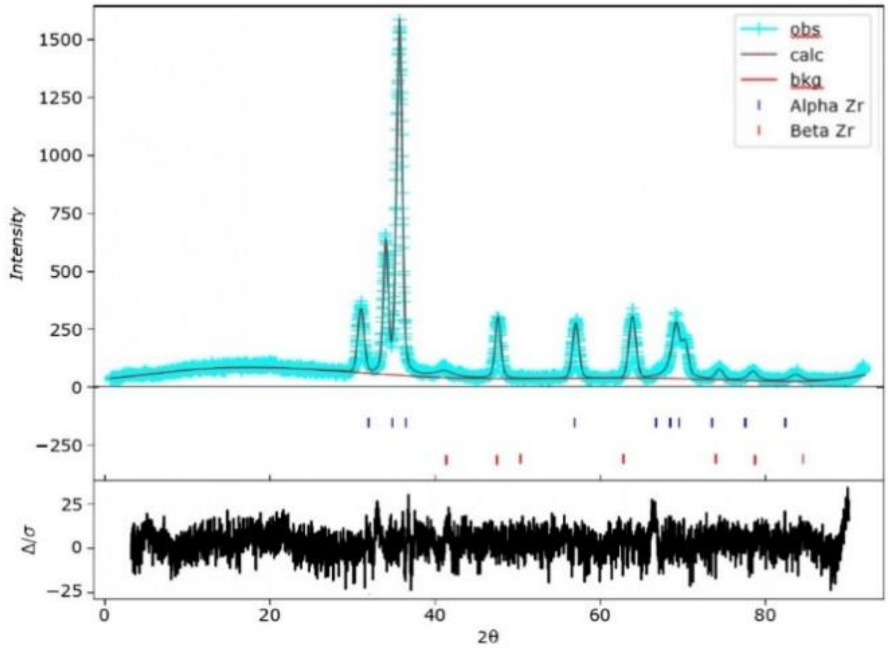

Figure 8. XRD results of the 5% Co sample, analysed by Rietveld using GSAS II software

Table 4. Sample weight fraction Zr92%Ag3%Co5% %

Phase	% Fraction
Alpa Zr	52.6%
Beta Zr	47.4%

Furthermore, the second sample, namely Zr90.5%Ag2%Co7.5%, is the same as the first sample; the second sample is processed by casting at a temperature of 2000℃ for 10 minutes with cooling for 15 minutes. The results of Rietveld refinement using GSAS-II (Figure 9).

Figure 9 shows that the second sample is better than the first sample, because more and more beta Zr phases are formed. The results of this second sample refinement show that the model used has a Goodness of Fit (GOF) = 1.67 and wR = 5.941. Meanwhile, the results of the calculation of the weight fraction are shown in Table 5.

Table 5. Sample weight fraction Zr90.5%Ag2%Co7.5%

Phase	% Fraction
Alpa Zr	37.2%
Beta Zr	62.8%

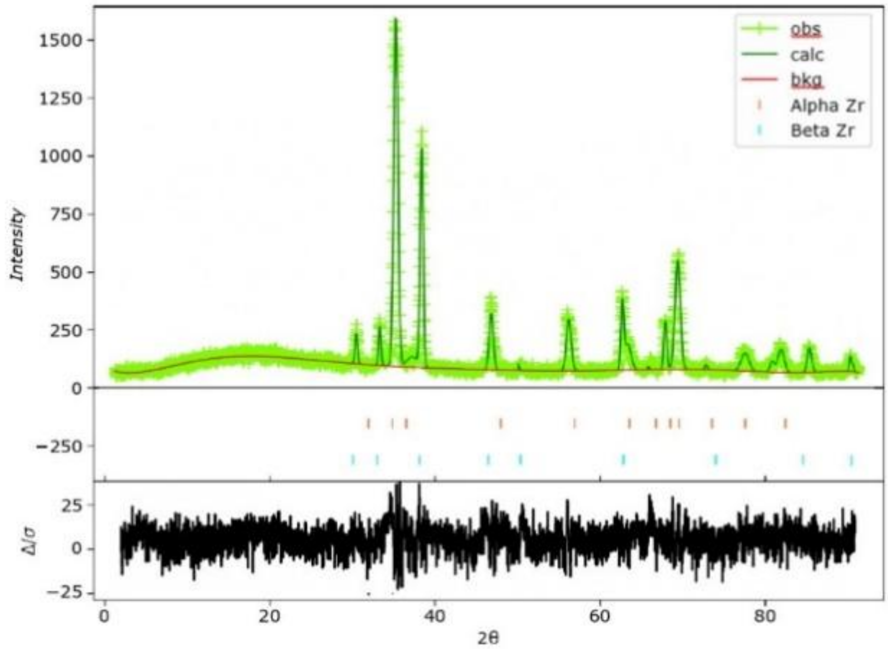

Figure 9. XRD results of the 7.5% Co sample, analysed by Rietveld using GSAS II software

Based on the results of the refinement and calculation of the weight fraction, it can be concluded that the synthesis of the ZrAg phase was reproducible. For a clearer comparison of the three samples can be seen in Fig. 10.

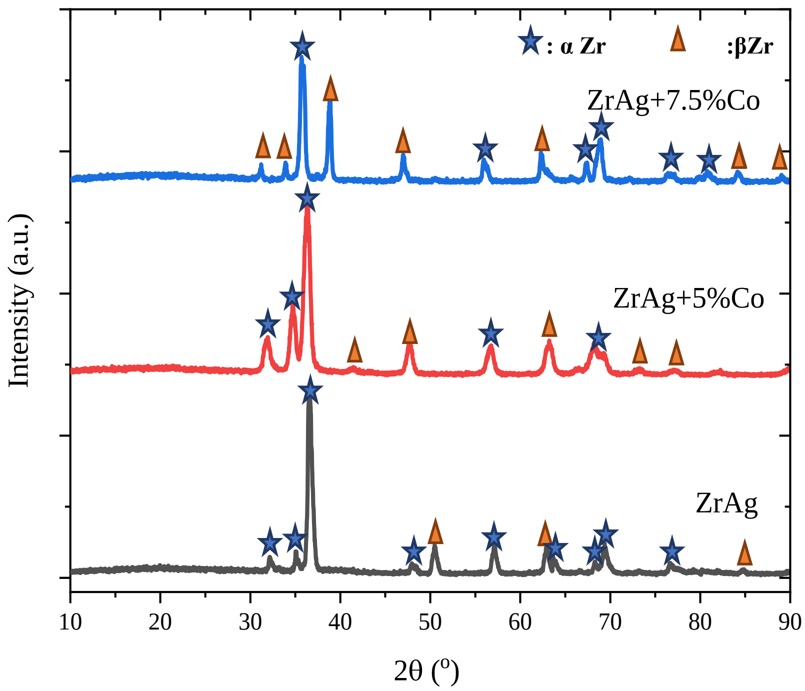

Figure 10. XRD comparison of the three ZrAg samples

All three samples have Alpha Zr forming a hexagonal structure with a P63/mmc space group, while the Beta Zr phase forms a cubic structure with an Im-3m space group with a general crystal structure. The scanning electron microscopy shows the different results of three samples of alloy (Figure 11).

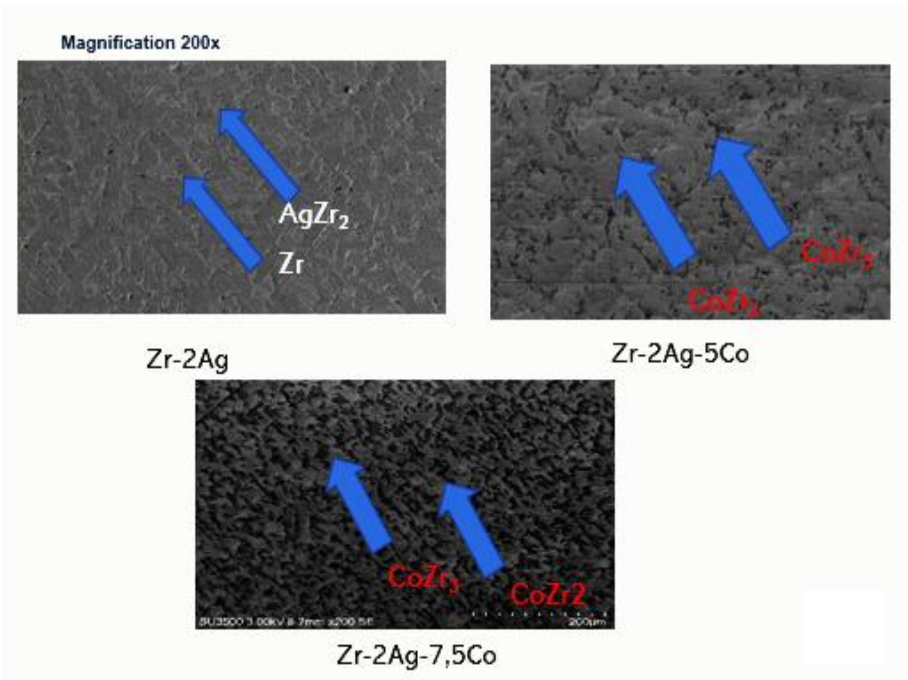

Figure 11. Scanning Electron Microscopy results

Zr-2Ag consists of a zirconium alloy with 2% silver. There are two main phases shown in the picture. The base Zr matrix and a secondary phase labelled $AgZr_2$, an intermetallic compound formed between silver and zirconium. The $AgZr_2$ appears as evenly distributed precipitates throughout the microstructure, indicating a relatively uniform solid-state reaction between the Ag and Zr. The presence of this phase can contribute to strengthening mechanisms such as precipitation hardening, potentially improving the mechanical properties like hardness and wear resistance without significantly disrupting the overall matrix structure. The relatively clean and homogeneous microstructure suggests minimal phase interaction or complexity, making this alloy a simple binary system ideal for basic strengthening with silver addition.

In Zr-2Ag-5Co, the alloying elements include 2% silver and 5% cobalt. The microstructure becomes more complex compared to the Zr-2Ag sample. Here, two additional intermetallic phases—$CoZr_2$ and $CoZr_3$—are identified, both formed between cobalt and zirconium. These new phases introduce significant changes to the morphology of the microstructure. The presence of Co appears to promote the nucleation of finer and more numerous intermetallic particles, possibly refining the grain structure. These Co-containing phases may influence not only the mechanical properties (through dispersion strengthening) but also affect corrosion resistance and thermal stability. The microstructural evolution demonstrates how Co alters phase formation and distribution in the Zr matrix beyond what Ag alone achieves.

Zr-2Ag-7.5Co combines a higher cobalt content—7.5%—alongside 2% silver. The micrograph shows an even denser and more intricate microstructure, with intermetallic phases labelled CoZr and $CoZr_2$. These phases, particularly CoZr, are typically harder and more stable than those seen in the lower-Co sample. The increase in cobalt concentration leads to more extensive formation of intermetallics, which are seen to occupy more of the matrix and appear more closely packed. This results in a more complex, less homogeneous appearance. The higher density of intermetallics can enhance mechanical strength, creep resistance, and thermal performance, but may also reduce ductility if the phases are overly brittle. This alloy represents a more advanced composition where the balance of strength and toughness must be carefully optimised.

4. Conclusion

The study indicates that the newly developed Zr-Ag-Co alloy shows promise as an alternative biomaterial for dental implant screws, although further investigation is required. The addition of cobalt (Co) into the Zr-2Ag alloy significantly enhances its hardness, with values increasing from 473.57 HV to 496.87 HV in the Zr-2Ag-5Co composition (a 5% improvement) and to 510.44 HV in the Zr-2Ag-7.5Co variant (a 3% rise). XRD and SEM confirm the formation of α-Zr, β-Zr, and intermetallic phases Zr_2Co, Zr_3Co, and Zr_2Ag. The presence of cobalt not only contributes to phase stability but also improves corrosion resistance. In Simulated Body Fluid (SBF), the corrosion rate decreased from 2.466 mpy in the base Zr-2Ag alloy to 2.115 mpy in the Zr-2Ag-5Co alloy, and further to 2.104 mpy in the Zr-2Ag-7.5Co alloy. Therefore, the Zr-2Ag-7.5Co shows the highest corrosion resistance.

References

[1] G. Spatafora, Y. Li, X. He, A. Cowan, and A. C. R. Tanner, “The Evolving Microbiome of Dental Caries,” *Microorganisms*, vol. 12, no. 1, p. 121, Jan. 2024, doi: https://doi.org/10.3390/microorganisms12010121.

[2] Y. Zhang, K. Gulati, Z. Li, P. Di, and Y. Liu, “Dental Implant Nano-Engineering: Advances, Limitations and Future Directions,” *Nanomaterials*, vol. 11, no. 10, p. 2489, Sep. 2021, doi: https://doi.org/10.3390/nano11102489.

[3] M. Panchal, S. Khare, P. Khamkar, and K. Suresh Bhole, “Dental implants: A review of types, design analysis, materials, additive manufacturing methods, and future scope,” *Mater. Today Proc.*, vol. 68, pp. 1860–1867, 2022, doi: https://doi.org/10.1016/j.matpr.2022.08.049.

[4] N. Jambhulkar, S. Jaju, A. Raut, and B. Bhoneja, “A review on surface modification of dental implants among various implant materials,” *Mater. Today Proc.*, vol. 72, pp. 3209–3215, 2023, doi: https://doi.org/10.1016/j.matpr.2022.12.022.

[5] A. Al-sanea, S. Aktas, T. Celik, and Y. Kisioglu, “Effects of the internal contact surfaces of dental implants on screw loosening: A 3-dimensional finite element analysis,” *J. Prosthet. Dent.*, vol. 130, no. 4, pp. 603.e1-603.e11, Oct. 2023, doi: 10.1016/j.prosdent.2023.07.007.

[6] A. M. Abraham and S. Venkatesan, “A review on application of biomaterials for medical and dental implants,” *Proc. Inst. Mech. Eng. Part L J. Mater. Des. Appl.*, vol. 237, no. 2, pp. 249–273, Feb. 2023, doi: https://doi.org/10.1177/14644207221121981.

[7] P. Lozano *et al.*, “Corrosion Behavior of Titanium Dental Implants with Implantoplasty,” *Materials (Basel).*, vol. 15, no. 4, p. 1563, Feb. 2022, doi: https://doi.org/10.3390/ma15041563.

[8] X. Zhou *et al.*, “Microstructural evolution and corrosion behavior of Ti–6Al–4V alloy fabricated by laser metal deposition for dental applications,” *J. Mater. Res. Technol.*,

vol. 14, pp. 1459–1472, Sep. 2021, doi: https://doi.org/10.1016/j.jmrt.2021.07.006.
[9] K. Lovera-Prado *et al.*, "Barbed Dental Ti6Al4V Alloy Screw: Design and Bench Testing," *Materials (Basel).*, vol. 16, no. 6, p. 2228, Mar. 2023, doi: https://doi.org/10.3390/ma16062228.
[10] N. Hossain *et al.*, "Recent development of dental implant materials, synthesis process, and failure – A review," *Results Chem.*, vol. 6, p. 101136, Dec. 2023, doi: https://doi.org/10.1016/j.rechem.2023.101136.
[11] P. Kadambi, P. Luniya, and P. Dhatrak, "Current advancements in polymer/polymer matrix composites for dental implants: A systematic review," *Mater. Today Proc.*, vol. 46, pp. 740–745, 2021, doi: https://doi.org/10.1016/j.matpr.2020.12.396.
[12] J. Neugebauer *et al.*, "Ceramic Dental Implants: A Systematic Review and Meta-analysis," *Int. J. Oral Maxillofac. Implants*, vol. 38, no. suppl, pp. 30–36, May 2023, 10.11607/jomi.10500.
[13] S. Saha and S. Roy, "Metallic Dental Implants Wear Mechanisms, Materials, and Manufacturing Processes: A Literature Review," *Materials (Basel).*, vol. 16, no. 1, p. 161, Dec. 2022, doi: https://doi.org/10.3390/ma16010161.
[14] I. Sailer, D. Karasan, A. Todorovic, M. Ligoutsikou, and B. E. Pjetursson, "Prosthetic failures in dental implant therapy," *Periodontol. 2000*, vol. 88, no. 1, pp. 130–144, Feb. 2022, doi: 10.1111/prd.12416.
[15] V. Srimaneepong *et al.*, "Fixed Prosthetic Restorations and Periodontal Health: A Narrative Review," *J. Funct. Biomater.*, vol. 13, no. 1, p. 15, Feb. 2022, doi: 10.3390/jfb13010015.
[16] Q. Zheng, L. Mao, Y. Shi, W. Fu, and Y. Hu, "Biocompatibility of Ti-6Al-4V titanium alloy implants with laser microgrooved surfaces," *Mater. Technol.*, vol. 37, no. 12, pp. 2039–2048, Oct. 2022, doi: https://doi.org/10.1080/10667857.2020.1816011.
[17] C. Cappellini, A. Malandruccolo, A. Abeni, and A. Attanasio, "A feasibility study of promoting osseointegration surface roughness by micro-milling of Ti-6Al-4V biomedical alloy," *Int. J. Adv. Manuf. Technol.*, vol. 126, no. 7–8, pp. 3053–3067, Jun. 2023, doi: 10.1007/s00170-023-11318-z.
[18] R. C. S. Silva *et al.*, "Titanium Dental Implants: An Overview of Applied Nanobiotechnology to Improve Biocompatibility and Prevent Infections," *Materials (Basel).*, vol. 15, no. 9, p. 3150, Apr. 2022, doi: https://doi.org/10.3390/ma15093150.
[19] A. M. A. Aljafery, A. A. Fatalla, and J. Haider, "Cytotoxicity, Corrosion Resistance, and Wettability of Titanium and Ti-TiB2 Composite Fabricated by Powder Metallurgy for Dental Implants," *Metals (Basel).*, vol. 14, no. 5, p. 538, May 2024, doi: https://doi.org/10.3390/met14050538.
[20] P. H. da H. Sales, A. W. P. Barros, O. B. de Oliveira-Neto, F. J. C. de Lima, A. de A. T. Carvalho, and J. C. Leão, "Do zirconia dental implants present better clinical results than titanium dental implants? A systematic review and meta-analysis," *J. Stomatol. Oral Maxillofac. Surg.*, vol. 124, no. 1, p. 101324, Feb. 2023, doi: 10.1016/j.jormas.2022.10.023.
[21] Y. Qu and L. Liu, "Zirconia Materials for Dental Implants: A Literature Review," *Front. Dent. Med.*, vol. 2, Aug. 2021, doi: https://doi.org/10.3389/fdmed.2021.687983.
[22] S. Ban, "Classification and Properties of Dental Zirconia as Implant Fixtures and Superstructures," *Materials (Basel).*, vol. 14, no. 17, p. 4879, Aug. 2021, doi: https://doi.org/10.3390/ma14174879.

[23] H. Lin, C. Yin, and A. Mo, “Zirconia Based Dental Biomaterials: Structure, Mechanical Properties, Biocompatibility, Surface Modification, and Applications as Implant,” *Front. Dent. Med.*, vol. 2, Aug. 2021, doi: https://doi.org/10.3389/fdmed.2021.689198.

[24] B. Huang, M. Chen, J. Wang, and X. Zhang, “Advances in zirconia-based dental materials: Properties, classification, applications, and future prospects,” *J. Dent.*, vol. 147, p. 105111, Aug. 2024, doi: https://doi.org/10.1016/j.jdent.2024.105111.

[25] N. Kumari *et al.*, “Zirconia-based nanomaterials: recent developments in synthesis and applications,” *Nanoscale Adv.*, vol. 4, no. 20, pp. 4210–4236, 2022, doi: https://doi.org/10.1039/D2NA00367H.

[26] F. Alkhudhairy and M. H. AlRefeai, “Self-Etch Adhesive-Loaded ZrO2/Ag3PO4 Nanoparticles on Caries-Affected Dentin: A Tensile Bond Strength, Scanning Electron Microscopy, Energy Dispersive X-ray Spectroscopy, Survival Rate Assessment of S. mutans, and Degree of Conversion Analysis,” *Appl. Sci.*, vol. 14, no. 2, p. 563, Jan. 2024, doi: https://doi.org/10.3390/app14020563.

[27] S. K. Mallineni *et al.*, “Silver Nanoparticles in Dental Applications: A Descriptive Review,” *Bioengineering*, vol. 10, no. 3, p. 327, Mar. 2023, doi: https://doi.org/10.3390/bioengineering10030327.

[28] S. K. Taha, E. A. Hassan, G. T. El-Bassyouni, S. Mousa, H. N. Shalash, and M. A. Abdel Hamid, “Evaluation of osseous healing in induced mandibular defects grafted with biphasic calcium phosphate doped with silver and zirconium nanoparticles: An experimental study in dogs,” *J. Oral Maxillofac. Surgery, Med. Pathol.*, vol. 36, no. 4, pp. 493–506, Jul. 2024, doi: https://doi.org/10.1016/j.ajoms.2023.12.002.

[29] M. Peng, J.-L. Chuan, G. Zhao, and Q. Fu, “Construction of silver-coated high translucent zirconia implanting abutment material and its property of antibacterial,” *Artif. Cells, Nanomedicine, Biotechnol.*, vol. 51, no. 1, pp. 441–452, Dec. 2023, doi: https://doi.org/10.1080/21691401.2023.2244013.

[30] D. Rokaya *et al.*, “Metallic Biomaterials for Medical and Dental Prosthetic Applications,” in *Functional Biomaterials*, Singapore: Springer Singapore, 2022, pp. 503–522. doi: 10.1007/978-981-16-7152-4_18.

[31] J.-B. Feng, R. Chen, B. Li, B.-H. Jiang, and B. Li, “The Current Trend of Antibacterial Prostheses and Prosthetic Surface Coating Technologies to Prevent Prosthetic Joint Infection for Artificial Joint Replacement,” *J. Biomater. Tissue Eng.*, vol. 13, no. 11, pp. 1046–1060, Nov. 2023, doi: https://doi.org/10.1166/jbt.2023.3342.

[32] A. Upadhyay, L. Pradhan, D. Yenurkar, K. Kumar, and S. Mukherjee, “Advancement in ceramic biomaterials for dental implants,” *Int. J. Appl. Ceram. Technol.*, vol. 21, no. 4, pp. 2796–2817, Jul. 2024, doi: 10.1111/ijac.14772.

[33] M. El-Telbany and A. El-Sharaki, “Antibacterial and anti-biofilm activity of silver nanoparticles on multi-drug resistance pseudomonas aeruginosa isolated from dental-implant,” *J. Oral Biol. Craniofacial Res.*, vol. 12, no. 1, pp. 199–203, Jan. 2022, doi: https://doi.org/10.1016/j.jobcr.2021.12.002.

[34] R. N. Salaie, P. A. Hassan, Z. D. Meran, and S. A. Hamad, “Antibacterial Activity of Dissolved Silver Fractions Released from Silver-Coated Titanium Dental Implant Abutments: A Study on Streptococcus mutans Biofilm Formation,” *Antibiotics*, vol. 12, no. 7, p. 1097, Jun. 2023, doi: https://doi.org/10.3390/antibiotics12071097.

[35] Y. Zhao, J. Xu, Q. Wang, Z.-H. Xie, and P. Munroe, “(TiZrNbTaMo)N nanocomposite coatings embedded with silver nanoparticles: imparting mechanical, osteogenic and antibacterial traits to dental implants,” *J. Alloys Compd.*, vol. 972, p. 172824, Jan. 2024, doi: https://doi.org/10.1016/j.jallcom.2023.172824.